Lignin Composites with Sustained Oxygenation and Reactive Oxygen Species-Scavenging Improve Neovascularization and Healing of Diabetic Wounds

Oluyinka O. Olutoye II[1*], Benjamin W. Padon[1*], Walker D. Short[1], Aditya A. Kaul[1], Lane D. Yutzy[2], Fayiz Faruk[1], Sonya S. Keswani[1], Olivia S. Jung[1,2], Phillip Kogan[1], Ling Yu[1], Hui Li[1], Jangwook P. Jung[2,#], Swathi Balaji[1,#]

[1]Division of Pediatric Surgery, Department of Surgery, Texas Children's Hospital and Baylor College of Medicine, Houston, TX
[2]Department of Biological Engineering, Louisiana State University, Baton Rouge, LA

*****Equal contribution

#Corresponding authors:
Swathi Balaji, Ph.D.
Texas Children's Hospital and Baylor College of Medicine
Feigin Center, C.450.05
1102 Bates Ave.
Houston, TX 77030
Phone: (832) 824-0461
Fax: (832) 825-3141
Email: balaji@bcm.edu

Jangwook P. Jung, Ph.D.
Louisiana State University
Department of Biological Engineering
167 E.B. Doran Hall
Baton Rouge, LA 70803
Phone: (225) 578-2919
Fax: (225) 578-3492
E-mail: jjung1@lsu.edu

Abbreviations

ROS - Reactive Oxygen Species
db/db - B6.BKS(D)-Leprdb/J
HIF-1α- Hypoxia inducible factor 1-alpha
ECM - Extracellular matrix
O_2 - Oxygen
IL-1Beta - Interleukin-1β
3D - Three dimensional
TLS - Thiolated lignosulfonate
SLS - Sodium lignosulfonate
CPO - Calcium peroxide containing lignin composite
CPOc – Calcium peroxide control containing lignin composite
H_2O_2 - Hydrogen peroxide
MPA - 3-mercaptopropionic acid
PLGA - Poly(lactic-co-glycolic) acid
PDI - Polydispersity index
GelMA – Methacrylated Gelatin
PBS - Phosphate buffered saline
LAP - Lithium phenyl-2,4,6-trimethylbenzoylphosphinate photo-initiator
UV - Ultraviolet
FBS - Fetal Bovine Serum
VEGF - Vascular endothelial growth factor
RNAse - Ribonuclease
RNA - Ribonucleic acid
ELISA - Enzyme-linked immunosorbent assay
PECAM - Platelet endothelial cell adhesion molecule
ABC-DAB - 3,3′-Diaminobenzidine
WES - automated capillary-based immunoassay system
ANOVA - Analysis of variance
H&E - Hematoxylin and eosin
MVEC - Murine microvascular endothelial cells
PDGF - Platelet-derived growth factor
HPF – High power field

ABSTRACT

Although delayed wound healing is an important clinical complication in diabetic patients, few targeted treatments are available, and it remains challenging to promote diabetic wound healing. Impaired neovascularization is one of the prime characteristics of the diabetic phenotype of delayed wound healing. Additionally, increased levels of reactive oxygen species (ROS) and chronic low-grade inflammation and hypoxia are associated with diabetes, which disrupts mechanisms of wound healing. We developed lignin composites with multiple wound healing-promotive functions, including pro-angiogenesis, sustained oxygenation from calcium peroxide (CaO_2)-based oxygen releasing nanoparticles and ROS–scavenging with thiolated lignosulfonate that captures the elevated ROS in diabetic wounds. The sustained release of oxygen and ROS-scavenging by the lignin composites promoted endothelial cell branching and their reorganization into characteristic network formation *in vitro*, promoted angiogenic growth factor expression and angiogenesis in full thickness skin wounds tested in a diabetic murine model of delayed wound healing, and decreased hypoxia inducible factor-1α (HIF-1α) expression. These effects significantly increased the granulation tissue deposition and tissue repair. Our findings demonstrate that lignin composites promote diabetic wound healing without use of other drugs and show the potential of functionalized lignosulfonate for wound healing applications requiring balanced antioxidation and controlled oxygen release.

INTRODUCTION

Over eight million people suffer from non-healing wounds every year in the United States [1, 2].Chronic wounds with impeded healing occur either due to infection or underlying conditions such as obesity, diabetes or aging, which are on the rise [3]. Recurrence of wounds in diabetic patients due to poor healing significantly increases their morbidity, risk for amputations, and mortality [4], and diabetes-related lower extremity complications are among the top 10 leading causes of the global burden of disability.

While acute, physiologic wounds progress through a series of wound healing stages of coagulation, inflammation, migration and proliferation, and remodeling, diabetic wounds are known to deviate from this wound healing pattern [5]. Diabetic wounds have a reduced ability to mount the effective immune response required for pathogen control due to reduced migration of leukocytes, neutrophils, and macrophages to the wound [6, 7]. The accumulation of advanced glycation end products in diabetic wounds increases reactive oxygen species (ROS) formation and reduction of macrophage efferocytosis, thereby impinging their ability to transition to M2 (alternatively activated) phenotype and impairing inflammation resolution [8]. This results in increased proteolytic activity along with a decrease in proteolysis inhibitors [9], culminating in insufficient accumulation of granulation tissue and neovascularization. Recent evidence further links excessive production of ROS and/or impaired detoxification of ROS to the pathogenesis of chronic wounds [10-12].

ROS are essential regulators of the wound healing process, as they facilitate defense against invading pathogens, and at low levels, are necessary for cellular functions such as proliferation, migration, and apoptosis [13]. ROS are produced as a result of normal cellular respiration, mitochondrial electron transfer chain [14], nicotinamide adenine dinucleotide

phosphate, nitric oxidase enzyme, and myeloperoxidase. Excess ROS are scavenged by enzymes such as superoxide dismutase and antioxidants that regulate the redox environment in healing skin wounds. However, excess ROS accumulation disrupts cellular homeostasis and causes non-specific damage to critical cellular components and function, leading to impairment such as abberant fibroblast collagen synthesis [15] and cell apoptosis. Antioxidants scavenge or neutralize free radical formation and inhibit the deleterious downstream effects of ROS, which can serve as potential therapeutic interventions to fight oxidative stress [16-23]. Strategies including nanoparticles made up of inorganic materials such as mesoporous silica, cerium oxide, and fullerene which exhibit antioxidant activities, have been evaluated *in vitro* and in animal models to determine their ability to scavenge free radicals and decrease ROS concentrations to protect cells against oxidative stress [24-27]. However, most antioxidants, taken orally, have limited absorption profile, leading to low bioavailability and insufficient concentrations at the target site [28, 29].

Toward the goal of tissue regeneration, ROS-responsive biomaterials have been identified as a type of promising therapeutic avenue to alleviate oxidative stress in tissue microenvironments [30]. Engineered biomaterials can also address the issue of the wound exudates that make healing a challenge, because incessant release of elevated levels of exudates in chronic wounds promote microbial infection and free radicals that oxidize biomolecules and activate the inflammatory-extracellular matrix (ECM) production cascades. We and others have shown that hydrogels create a provisional wound matrix with good biocompatibility, nutrient supply, and swelling that allows absorption of excess exudates and maintenance of optimal moisture [31-35]. Thus, appropriate design of these biomaterials renders resistance to excess wound hydrolysis and can provide missing cues such as antioxidation and ROS scavenging,

thereby jump-starting healing by redirecting the wounds from the state of inflammation to the next stages. Furthermore, when large wounds are considered, lack of nutrient supply and oxygen generation beyond the limits of diffusion in tissue (100 to 200 μm) have been a major limiting factor for biomaterial-based therapies [36]. These deficiencies and the simultaneous disruption of several pathways involved in diabetic wound healing response may in part explain why some of the current therapies to treat diabetic wound healing are not entirely successful. Therefore, we aimed to address this gap by altering the diabetic wound microenvironment with novel lignin-based composites.

Lignin is a polyphenolic polymer that can isolate pathogens to the site of infection while providing imperviousness to cell walls in vascular plants [37]. The use of lignin in wound-healing dressings is an emerging field [38], with proven effects as an antiviral [39],[40], and for its antioxidation, immunostimulation [41] and anticoagulation [42] properties. In addition, the enhanced mechanical properties [43] with good protein adsorption capacity and wound compatibility [44] of this natural polyphenolic molecule, along with its anti-inflammatory properties, such as its capacity to reduce gene expression of iNOS and IL-1β of inflamed macrophages [45], and enhanced biocompatibility without toxicity [46] are promising for wound healing applications. Previous studies showed that lignin treatment improved mechanical properties and wound healing of incision wounds in Sprague-Dawley rats [47]. Not surprisingly, the majority of applications of lignin-based biomaterials take advantage of its antioxidation property [17, 48-56]. Review of relevant literature shows that the primary mode of application of lignin to wounds is via entrapment or complexation for rapid release of nanoparticles. Thus, we have sought to apply lignin in this study, topically, to diabetic wounds. We have produced a novel, dual action lignosulfonate-composite biomaterial incorporating 1) thiolated lignosulfonate

(TLS) nanoparticles for antioxidation [57] and 2) sodium lignosulfonate (SLS)-based, calcium peroxide nanoparticles (termed CPO) for controlled release of oxygen, that not only scavenges reactive oxygen species but also produces oxygen without increasing detrimental byproducts (i.e. H_2O_2), to serve as a correcting, provisional matrix for diabetic wounds. We hypothesized that optimal lignin composite constituents will improve release of beneficial oxygen and antioxidation to the infiltrating cells, resulting in improved neovascularization and granulation tissue, necessary for improved healing and tissue regeneration in murine diabetic wounds.

METHODS

Synthesis of Lignin Composites

To produce TLS, sodium lignosulfonate (SLS, TCI Chemicals) was functionalized with 3-mercaptopropionic acid (MPA) in hydrochloric acid [57]. We confirmed that the thiolation is dominant on aliphatic hydroxide of SLS and the extent of thiolation of TLS was tunable by modulating stoichiometry of MPA [57]. The coupling of lignosulfonate to PLGA (poly(lactic-*co*-glycolic) acid) was performed by acylation reaction for SLS [58] in a mass ratio of 2 to 1. SLS-*graft*-PLGA and CaO_2 were dissolved in ethyl acetate (organic phase) under stirring at room temperature. The suspension was homogenized with a microfluidizer (Microfluidics Corp., Westwood, MA) at 30 kpsi at 4°C. Next, the organic solvent was evaporated with a rotary evaporator R-300 (Buchi Corp, New Castle, DE). Finally, trehalose was added (1:1 mass ratio) as a cryoprotectant for SLS:PLGA nanoparticle lyophilization and stored at -20°C for further characterization and tests.

Precursors of lignin composites were reconstituted in 1 mg/mL LAP (Lithium phenyl-2,4,6-trimethylbenzoylphosphinate) in PBS. The final concentrations were 50 mg/mL gelatin

methacrylate (GelMA) [57, 59] with TLS (3 mg/mL) plus either CPOc (4 mg/mL, CPO control – SLS particles formed without CaO_2) or CPO (4 mg/mL, SLS particles formed with CaO_2). Precursors were cast into custom molds or topically applied in db/db mouse wounds followed by UV illumination for 60 s (365 nm) for gelation of the lignin composites in situ.

Assessment of Capillary-like Network Formation of MVECs

Murine dermal microvascular endothelial cells (MVECs) were purchased from Cell Biologics and cultured in T-25 flasks coated with 0.1% gelatin (Boston Bioproducts, Milford, MA). Control MVECs were cultured in Endothelial Cell Medium (Sciencell, Carlsbad, CA) with 5% FBS, while MVECs in the test group were treated with 30 mM dextrose in Endothelial Cell Medium with 5% FBS. MVECs in the test group were cultured in 30 mM dextrose for 5-7 days prior to the tube formation assay. On the night prior to the assay, both control and test MVECs were cultured under the previously stated conditions but with Endothelial Cell Medium containing only 1% FBS for cell starvation. On the day of the assay, 50 µL of lignin composites were cast into a custom polydimethylsiloxane (PDMS) well (8 mm diameter and 1 mm height) fixed on a glass slide to prevent meniscus formation. Four groups of lignin composites were cast, 1) GelMA, 2) GelMA + TLS, 3) GelMA + TLS + CPOc, and 4) GelMA + TLS+ CPO (abbreviation of lignin composites in **Table 1**). The precursors of lignin composites were then photopolymerized under UV light for 60 s. The hydrogels were washed with PBS twice. MVECs were seeded onto the lignin composites at 5.0×10^4 cells per well. The MVECs were then placed in a CO_2 incubator (37°C/5% CO_2). A set of randomly selected five phase contrast images were taken per each composite using an inverted fluorescence microscope (Nikon Eclipse Ti2) and NIS Elements Advanced Research Microscope Imaging Software (NIS Elements AR, Nikon) at

every 24 h over 96 h. Angiogenesis Analyzer [60] in FIJI software was used to assess the capillary-like network formation with the seven relevant-features of angiogenesis discussed in the results.

Table 1. Abbreviation of lignin composites

Abbreviation	Matrix	Nanoparticles (NPs)
UNTX	None	None
GelMA	GelMA	None
TLS	GelMA	TLS
CPOc	GelMA	TLS and SLS-PLGA (w/o CaO_2)
CPO	GelMA	TLS and SLS-PLGA/CaO_2

Assessment of VEGF and HIF-1α Protein Expression in Cultures of MVECs

Following the imaging for network formation of MVECs, supernatant was collected at every 24 h over 96 h, and protease and phosphatase inhibitors were added to the conditioned medium before freezing at -80°C. Expression levels of murine vascular endothelial growth factor (VEGF) (Quantikine ELISA kit, R&D Systems, Minneapolis, MN, USA) and HIF-1α (SimpleStep ELISA kit, Abcam ab275103, Cambridge MA, USA) were determined in the culture medium using ELISA as per manufacturers' protocols. Optical density was read on a BioTek Gen5 ™ Microplate Reader and standard curves were generated to determine cytokine concentrations using Imager Software.

In Vivo Model of Diabetic Wound Healing

A mouse model of diabetic wound healing was used to validate that the *in vitro* results of angiogenic responses of MVECs on lignin composites can be translated to improved healing in *in vivo* diabetic wound conditions. This model is characterized by a delayed wound healing with

reduced neovascularization [61] and increase in ROS and inflammation. All procedures were approved by the Institutional Animal Care and Use Committee. Eight-week-old female, diabetic B6.BKS(D)-*Lepr*^{db}/J (db/db) mice were obtained from Jackson Laboratories (Bar Harbor, ME). Two full thickness 6 mm circular excisional wounds were created side-by-side on the bilateral flanks on the dorsum of each animal, leaving the underlying muscle (panniculus carnosus) intact, as previously described [61]. A silicone stent was sutured around the wound with inner diameter of 8 mm to prevent wound contraction of loose skinned murine wounds. A sterile transparent dressing Tegaderm^{3M}, was applied to the skin to cover the wounds and held in place with benzoin tincture. Lignin composites containing 1) GelMA + LAP, 2) GelMA + LAP + TLS, 3) GelMA + LAP + TLS + CPOc, and 4) GelMA + LAP + TLS+ CPO (n=3, per each group), were injected into one wound immediately after wounding. The PBS treatment on the other-side wound served as an internal control for every animal. The animals were euthanized at days 7 and 14; wound tissues were harvested, fixed, and paraffin embedded.

Immunohistochemistry

Skin tissue was harvested, fixed in 10% neutral buffered formalin and paraffin embedded. 5 µm thick sections were cut and mounted onto superfrost plus slides. Slides were deparaffinized and rehydrated to PBS following standard protocol and immunohistochemistry staining was performed on a Dako Auto-stainer Link 48 (DakoLink version 4.1, edition 3.1.0.987; Agilent, Santa Clara, CA). Primary antibodies against CD31 for endothelial cells (ab28364; 1:100; Abcam, Cambridge, MA), VEGF (MA5-3208; 1:300, Thermofisher Scientific, Waltham, MA), HIF-1α (ab179483; 1:100; Abcam, Cambridge, MA), CD45 for pan-leukocytes (ab10558; 1:5000; Abcam, Cambridge, MA), F4/80 for pan-macrophages (ab111101; 1:100; Abcam,

Cambridge, MA) and cytokeratin 14 for basal keratinocytes (ab181595; 1:250; Abcam) were applied followed by detection using an EnVision+System-HRP (DAB) kit (Dako North America, Carpinteria, CA) and hematoxylin counter staining. Histology slides were imaged with Leica DM 2000® with Leica Application Suite X® version 3.0.4.16529. Percentage of positive cells and capillary lumens per high powered field (HPF) (40x) within the granulating wound bed were quantified in 6 random fields distributed along the wound bed.

Quantification of VEGF and HIF-1α in the Wound Homogenates

To determine protein expression of VEGF and HIF-1α in the db/db mice wounds treated with different lignin composites, wounds at day 7 post wounding were harvested. 10-50 mg each of the wound tissues were homogenized in 300 µL of freshly prepared RIPA buffer (Thermo Fisher Scientific 89900, Waltham, MA, USA). The digested samples were centrifuged and only the top supernatant was used in the quantification of expression levels of murine VEGF (Quantikine ELISA kit, R&D Systems, Minneapolis, MN, USA) and HIF-1α (SimpleStep ELISA kit, Abcam ab275103, Cambridge MA, USA) as per manufacturers' protocols. Optical density was read on a BioTek Gen5 ™ Microplate Reader and standard curves were generated to determine cytokine concentrations using Imager Software.

Statistical Analyses

Statistical comparisons between groups were performed by one-way ANOVA. For multiple comparisons, one-way ANOVA with Tukey's *post hoc* comparison was carried out. p values at least <0.05 were considered statistically significant. All bar graphs represent mean ± standard deviation (SD).

RESULTS

Endothelial capillary-like network formation was improved on dual acting lignin composites.

Following 5 days of treatment with 30 mM glucose in 2D cultures, MVECs were seeded onto lignin composites, GelMA, TLS, CPOc and CPO (see **Table 1** for details of abbreviations) up to 96 h. Phase contrast micrographs were taken and analyzed using Angiogenesis Analyzer [60]. As shown in **Figure 1**, lignin composites supported the growth and capillary-like network formation of MVECs. Seven features were selected from the Angiogenesis Analyzer including number of extremities, number of nodes, number of junctions, number of branches, number of isolated segments, sum of isolated branch lengths, and average mesh sizes (**Figure 2**). Lignin composites improved the characteristic capillary-like angiogenesis features in both normal and high glucose (oxidative stress) conditions. These features were significantly higher in CPO lignin composite hydrogels in the presence of high glucose, while those in normal glucose conditions only showed marginal improvements over the GelMA control.

VEGF and HIF-1α expression of MVECs was altered *in vitro* in lignin composites.

VEGF and HIF-1α are two important growth factors involved in neovascularization of the wounds, and they are also highly susceptible to ROS-mediated variations in the wound milieu that ultimately guide angiogenic responses. Hence, we sought to determine their expression in both control and test group of MVECs cultured in normal and high glucose conditions. HIF-1α was expressed highest in the supernatant of high glucose MVECs on the GelMA (353.4 pg/mL). The MVECs on the TLS, CPOc and CPO had a downward trend of HIF-1α expression with CPO being the lowest at 243.4 pg/mL. This same trend was present in

control MVECs, though with lower values as compared to those under high glucose conditions (GelMA: 276.1 pg/mL, TLS: 272.7 pg/mL, CPOc: 256.2 pg/mL, CPO:248.3 pg/mL) **(Figure 3A).** Compared to control cells, VEGF expression increased in MVECs under high glucose conditions. VEGF was expressed highest in the supernatant of high glucose MVECs on the GelMA (30.1 pg/mL). Compared to the GelMA condition, VEGF expression in the supernatant of high glucose MVECs was relatively decreased, though not significantly on TLS (17.5 pg/mL), CPOc (19.0 pg/mL), and CPO (16.4 pg/mL). This same trend was seen in the supernatant of control MVECs (**Figure 3B).**

Antioxidant, oxygen-generating dual acting lignin composites improved wound closure, and granulation tissue and capillary lumen formation in db/db wounds at day 7.

We evaluated wound healing in 8-week-old diabetic (db/db) mice with blood glucose >350 mg/dl. 6 mm wounds (**Figure 4A**) were treated with lignin composites, TLS, CPO or CPOc immediately after wounding on day 0, and their healing was compared to untreated wounds (UNTX). Cytokeratin staining to assess the epithelial gap (distance between the encroaching epithelial margins) showed reduced epithelial gap in the CPO wounds at day 7 as compared to other treatments (UNTX: 4.67 ± 0.75 mm, TLS: 4.33 ± 1.34 mm, CPOc: 3.15 ± 0.94 mm, CPO: 3.22 ± .56 mm) **(Figure 4B** and **C).** These data indicate a notable trend with improvement in wound morphology of dual acting, CPO lignin composite-treated wounds. However more animals are needed to achieve better statistical significance. Further, wounds treated with CPO had significantly more granulating tissue present at day 7 as compared to other treatments (Untreated: 0.5 ± 0.1 mm^2, TLS: 0.6 ± 0.4 mm^2, CPOc: 0.4 ± 0.2 mm^2, CPO: 1.7 ± 0.8 mm^2) (**Figure 4D**).

CD31 staining of wound sections collected at day 7 showed a significant increase in capillary lumen density in CPO treated wounds (11 ± 1.2 vessels/HPF), as compared to UNTX (6 ± 0.1 vessels/HPF, $p<0.01$), TLS (6 ± 1.7 vessels/HPF, $p=0.02$), and CPOc (6 ± 2.4 vessels/HPF, $p=0.049$) **(Figure 5A** and **D)**. Interestingly, we noted striking differences in VEGF and HIF-1α expression with immunohistochemistry at the leading epidermal margins in CPO vs. other treatments. Consistent with previous literature on normal wound healing in murine skin wounds, db/db mice leading epidermal edges in UNTX wounds displayed abundant VEGF and HIF-1α staining at day 7 post wounding, which is upregulated in response to injury-induced oxidative stress **(Figure 5B** and **C)**. Similar expression patterns were noted in TLS and CPOc wounds. Strikingly, the oxygen generating lignin composite CPO did not elicit this response at day 7. Histological staining for VEGF and HIF-1α showed reduced expression in the hyperproliferative leading epidermis of CPO-treated wounds at day 7 post wounding. While immunohistochemical staining of VEGF was reduced in the epidermis, quantification of VEGF expression in the homogenized wound tissue using ELISA showed an increase in the VEGF expression at day 7 in the wound bed **(Figure 5E)**, suggesting dermal angiogenesis is promoted by CPO lignin composites. HIF-1α quantification of the homogenized wounds showed significantly reduced expression in CPO wounds at day 7 as compared to UNTX, TLS and CPOc wounds **(Figure 5F)**.

In addition, we did not see any significant difference in the expression of $CD45^+$ (pan-leukocyte) cells across all tested lignin composites as compared to untreated wounds at day 7. CD45 staining displayed a slight decreased in CPO wounds (13 ± 10 % $CD45^+$ cells/HPF) compared to untreated (24 ± 10 % $CD45^+$ cells/HPF, $p=0.26$), TLS (10 ± 2 % $CD45^+$ cells/HPF, $p=0.60$), and CPOc (16 ± 9 %$CD45^+$ cells/HPF, $p=0.72$) conditions, although this decrease was

not statistically significant **(Figure 6A** and **C)**. F4/80 staining displayed a significant decrease in macrophages in CPO-treated wounds compared to TLS-treated wounds (17 ± 2 % F4/80^{+}cells/HPF vs. 41 ± 6 % F4/80^{+}cells/HPF, $p<0.01$). F4/80 staining was decreased in CPO-treated wounds compared to both untreated (26 ± 12 % F4/80^{+}cells/HPF, $p=0.26$) and CPOc-treated (20 ± 10 % F4/80^{+}cells/HPF) wounds, however these differences did not reach significance **(Figure 6B** and **D)**, indicating minimal inflammatory response from CPO or CPOc nanoparticles in lignin composites.

CPO Lignin composites promoted capillary lumen formation and robust granulation tissue remodeling over 14 days in db/db wounds.

To determine the effect of the lignin composite treatment on remodeling in db/db wounds, we tested the effect of treatment at additional time point of 14 days post wounding. At day 14, we noted visibly improved healing in CPOc and CPO wounds from gross images, which was supported by the presence of a robust granulating wound bed in representative hematoxylin and eosin-stained wounds sections **(Figure 7A).** Day 14 wounds treated with CPO (24 ± 4 CD31^{+} lumens/HPF) also displayed significantly increased lumen density with CD31 staining compared to TLS (12 ± 5 CD31^{+} lumens/HPF) and CPOc (14 ± 2 CD31^{+} lumens/HPF) but did not approach significance compared to UNTX (19 ± 0.33 CD31^{+} lumens/HPF) **(Figure 7B** and **C)**.

DISCUSSION

Diabetes is known to activate the ROS system and inactivate antioxidation including enzymes such as superoxide dismutase [62, 63]. This leads to impaired wound healing [64-67]

via impairment of multiple pathways resulting in increased inflammation, decreased granulation tissue formation, and poor blood supply [68]. We sought to determine whether composites with lignosulfonates would promote diabetic wound healing by rescuing these effects of impaired ROS. We tested whether antioxidant and oxygen-generating lignin composites can promote endothelial cell functions under hyperglycemic conditions. We utilized murine MVEC from the skin and exposed them to high glucose (30 mM) for 5-7 days, and then cultured them on lignin composites of TLS, CPO, CPOc, and GelMA-only control. We noted a significant improvement in EC network formation with CPO **(Figure 1-2)**, suggesting that oxygen-generating lignin composites may correct cellular dysfunctions in diabetic endothelial cells. However, recent reports suggest that an *in vitro* acute hyperglycemic model may not be ideal for mechanistic studies of the effects of diabetes on EC responses, due to a phenomenon called "hyperglycemic memory" [69-73]. Thus, experimental evidence suggests that oxidative stress results in sustained activation of antiangiogenic, proinflammatory pathways in MVECs even after glycemia is normalized (i.e., the cell phenotype of endothelial cells becomes altered permanently, although the exact mechanisms are not well understood), as shown in our previous studies [34]. In addition, previous studies have shown an increase in VEGF expression in diabetic endothelial cells and those under excessive ROS, which was also noted in our cell culture experiments with MVEC under high concentration of glucose. Culture of these cells on the CPO lignin composites reversed these effects induced by high concentration of glucose [74, 75]. The important implication of these findings is that there is a need for novel therapies that can reverse hyperglycemic memory of endothelial cells to promote their cell-cell and cell-matrix interactions and neovascularization, a gap that could be filled with our lignin composite design.

We then harvested wounds from 8-week-old db/db mice with 6 mm wounds treated with lignin composites containing TLS, CPOc, or CPO. We found that the leading epidermal edges of all wounds in untreated, TLS- and CPOc-treatement exhibited HIF-1α induction, which is expected. However, when there were oxygen generating particles, as with CPO, we did not observe a significant upregulation of HIF-1α at the edges, though we do see granulation tissue improvement– signifying that the wound is indeed healing. This suggests that exogenous oxygen released into the wound alters hypoxia-induced pathways in diabetic wounds in a way that reduces HIF-1α expression at wound edges. Further understanding of these pathways leading to HIF-1α expression in diabetic mice treated with lignin composites will be the focus of future projects.

VEGF, which is well-known for its proangiogenic abilities [76, 77], also plays a significant role in cutaneous wound healing and has also been shown to be involved in hair growth [78], skin diseases [79-82], and cutaneous cancers [83, 84]. Interestingly, despite the known connection between HIF-1α and VEGF [85-87], we see that VEGF expression is increased at the wound edges of CPO-treated wounds, suggesting that CPO scavenges ROS in the wound and increases VEGF via pathways independent of HIF-1α. The mechanism by which this occurs is not well described and could be a future area of study, however, increased oxygen levels in diabetic wounds have previously been shown to increase wound VEGF levels. In a rat wound model, hyperbaric oxygen treatment resulted in increased VEGF in wound fluid [88]. We have shown that this increase in VEGF in CPO-treated wounds is accompanied by expected increase in capillary vessel density and improved wound healing. Further understanding of the role of the CPO lignin composites in the regulation of VEGF expression will help improve the design of our scaffolds to increase their wound healing efficacy.

Diabetic wounds are plagued by decreased granulation tissue formation [68], however, we see that granulation tissue was significantly improved at days 7 and 14 in the db/db mouse wounds with CPO. This robust granulation tissue formation in the CPO lignin composites suggests that scavenging the free radicals and ROS via lignin in the wound rescues the alterations caused by hyperglycemic memory and restores robust tissue formation. We do not yet know the mechanism by which this occurs, and it is an area of further research. Understanding of the pathways to this restoration of robust granulation tissue may give insight to improve diabetic wounds and decrease the incidence of wound recurrence.

There are several limitations to this study. We use the db/db mouse as a model for diabetic wounds. The excisional wounds were made manually rather than spontaneously as in diabetic wounds/ulcers on human skin. Additionally, contraction plays a significant role in healing of excisional wounds in the mouse model, in contrast to human skin, requiring stent placement to limit this effect as previously described [89, 90]. Pig models are a superior model for studying wound healing, as the skin architecture is akin to that of humans; thus, pig models will be used in future studies.

CONCLUSIONS

We have shown that ROS scavenging by the constitutes of lignin composites along with locoregional oxygen release decreases HIF-1α expression, increases VEGF expression, and increases granulation tissue formation in a wounded db/db mouse model. These data support the well-known notion that oxidative stress causes impaired wound healing and suggest an engineered solution for improving diabetic wound healing by increasing oxygen levels in the wound while simultaneously scavenging free radicals using our CPO lignin composite. Future

studies will be focused on data-driven optimization of the CPO lignin composite to further improve the diabetic wound microenvironment with the goal of transition to large animal studies and translation to human diabetic wounds.

AUTHOR CONTRIBUTIONS

JPJ and SB designed the experiments. SB, BWP, OOO, WDS, SSK, AAK conducted *in vitro* and animal experiments and analyzed the results. LDY and OSJ performed EC experiments with lignin composites. FF, OSJ, PK analyzed the wounds and endothelial networks. HL, SSK and LY performed cell culture and the molecular biology assays. SB, JPJ, OOO, WDS and BWP wrote the manuscript, and all authors approved the final manuscript.

ACKNOWLEDGMENTS

The authors acknowledge the support from Wound Healing Society Foundation FLASH and 3M Awards (SB), Clayton Award from the Department of Surgery, Texas Children's Hospital (SB), John S. Dunn Foundation Collaborative Research Award (SB), the National Science Foundation EPSCoR Track 2 RII, OIA 1632854 (JPJ), the National Science Foundation CAREER DMR 2047018 (JPJ), the LSU Faculty Research Grant (JPJ) and the Donald W. Clayton Scholarship from the LSU College of Engineering (LDY). The authors acknowledge Carlos E. Astete for the synthesis of CPO and CPOc nanoparticles.

DISCLOSURES

None

FIGURES

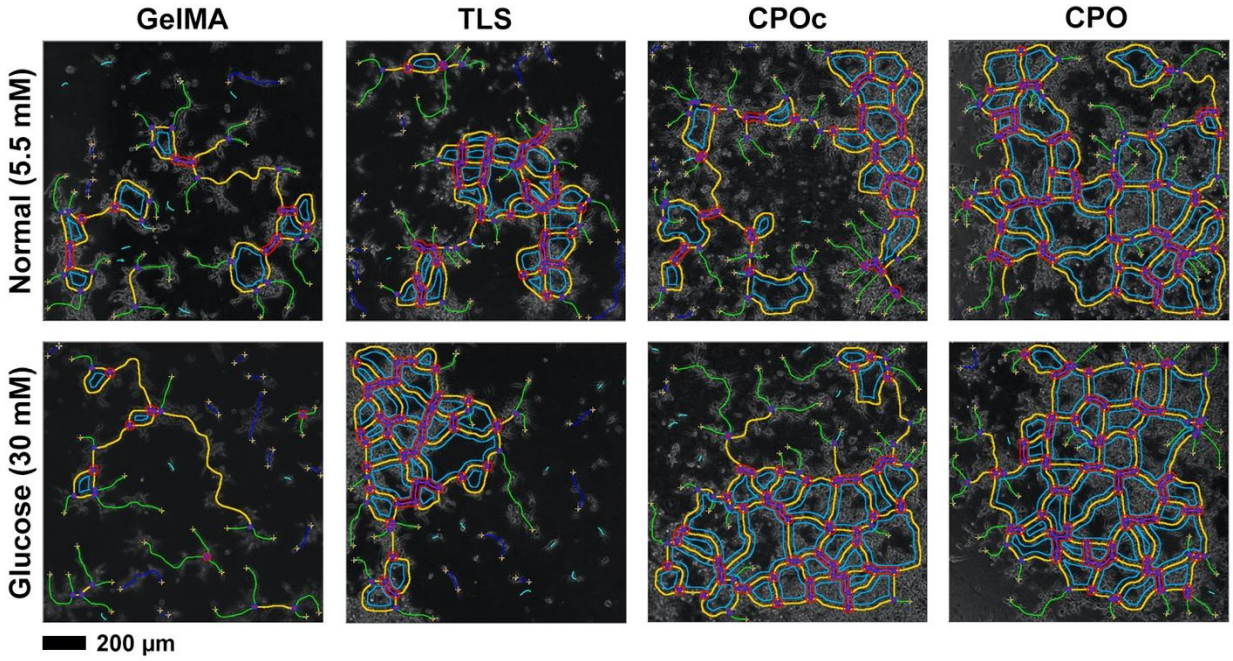

Figure 1. Representative results of Angiogenesis Analyzer [60] for the micrographs taken after 96 h of MVEC culture initiation. GelMA (50 mg/mL); TLS – GelMA 50 mg/mL with TLS 3 mg/mL; CPOc – GelMA 50 mg/mL with TLS 3 mg/mL and CPO nanoparticle 4 mg/mL without incorporating CaO_2; CPO - GelMA 50 mg/mL with TLS 3 mg/mL and CPO nanoparticle 4 mg/mL. Green - branches; Cyan - twigs and small isolated segments; Magenta - segment; Yellow/Orange - master segments; Sky blue - mesh; Dark blue - isolated elements.

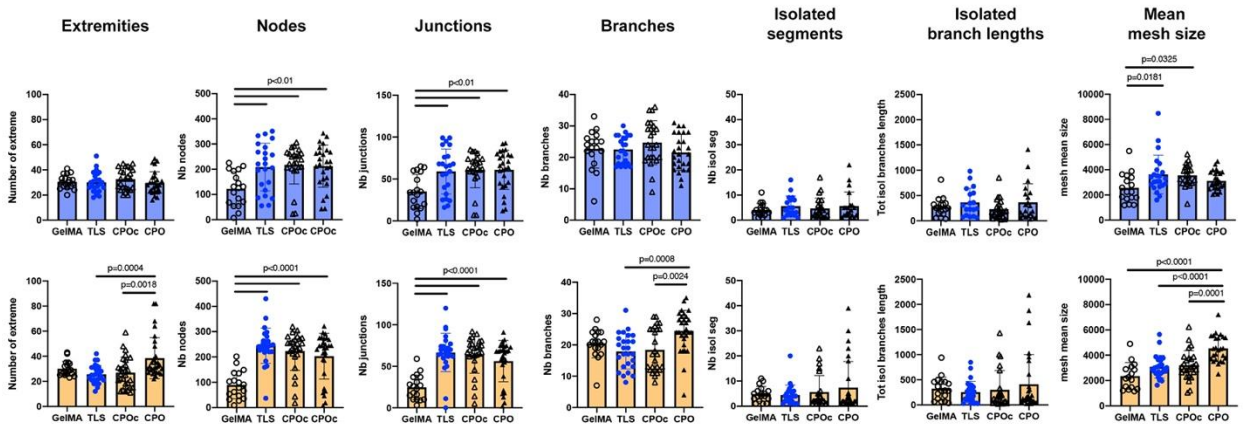

Figure 2. Seven angiogenic features were analyzed to assess the performance of lignin composites in two different conditions (blue, normal 5.5 mM glucose in the culture medium; orange, high glucose 30 mM glucose in the culture medium): number of extremities, number of nodes, number of junctions, number of branches, number of isolated segments, sum of isolated branch lengths, and average mesh sizes. Mean±SD, n=6-9 independent samples, 3 images/composite were analyzed. p values by one way ANOVA and Tukey's *post hoc* tests.

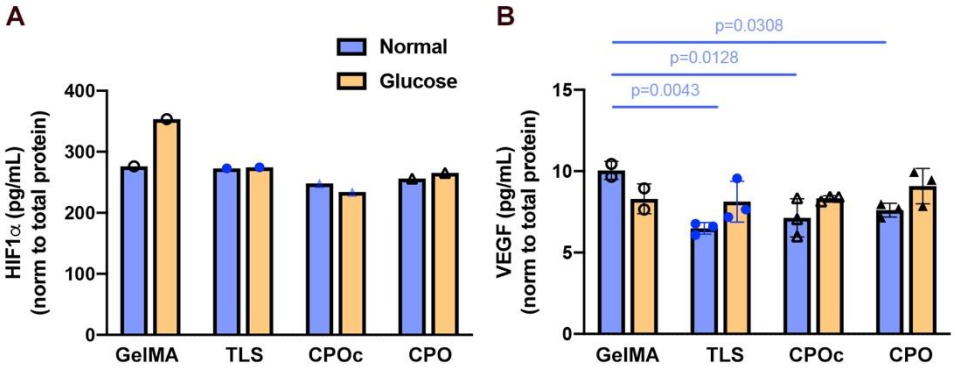

Figure 3. Analysis of levels of HIF-1α (A) and VEGF (B) collected in MVEC culture medium containing either normal (5.5 mM) glucose or high (30 mM) glucose. Mean±SD, n=2 or 3. p values by one way ANOVA Tukey's *post hoc* tests.

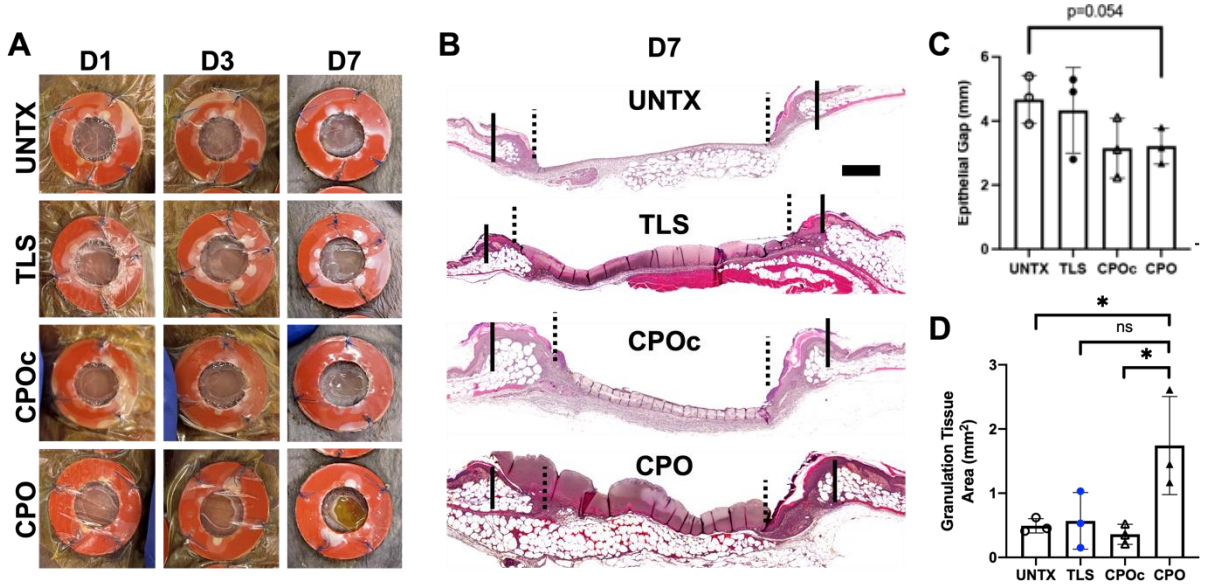

Figure 4. (A) Healing progression of db/db mouse wounds treated with lignin composite TLS, CPO or CPOc at 7 days post-wounding compared to UNTX wounds. (B) Gross images taken at indicated intervals post-wounding, with representative H&E staining of post-wounding day 7 wounds, Scale bar = 50 µm. Quantification of epithelial gap from cytokeratin stained wound sections (C), and granulation tissue area from H&E stained wound sections (D) at day 7 post wounding. Mean±SD, n=3 wounds per treatment group, *$p<0.05$ by one way ANOVA and Tukey's *post hoc* tests.

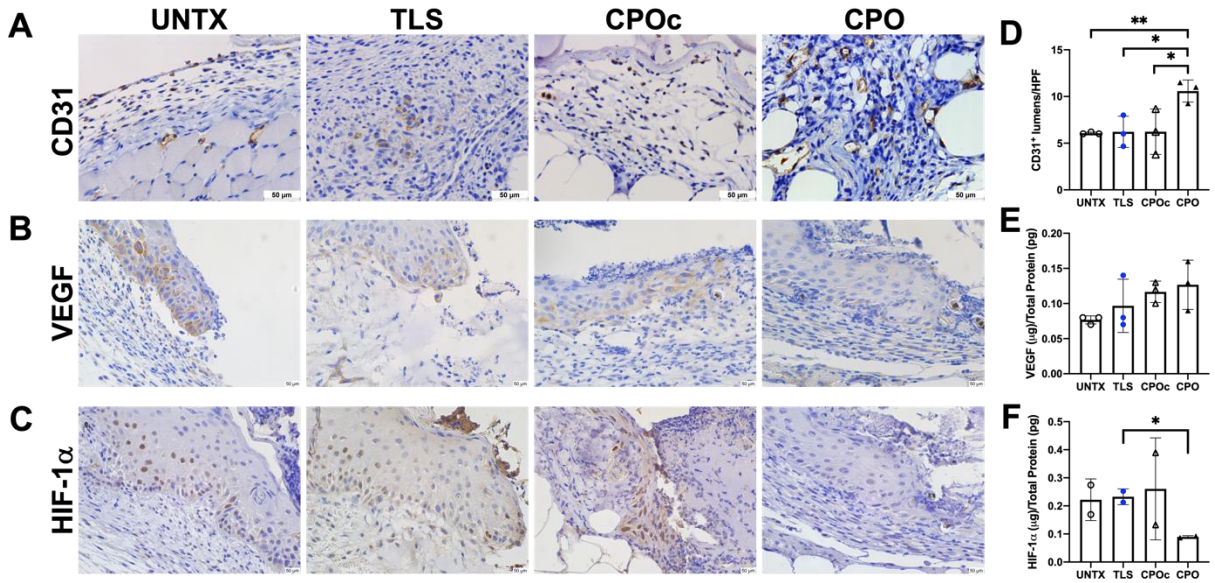

Figure 5. Neovascularization panel in db/db mouse wounds treated with lignin composite TLS, CPOc or CPO immediately post-wounding compared to UNTX wounds. Staining of day 7 wound sections with antibodies against CD31 (A), VEGF (B), and HIF-1α (C), Scale bar = 50 µm. (D) CD31 staining of wound sections showed a significant increase in lumen density per HPF in CPO wounds at day 7. Day 7 wound tissue homogenates evaluated using ELISA revealed an increasing trend of VEGF expression (E) and significantly decreased HIF-1α expression (F) in CPO wounds. Mean±SD, n=3 wounds per treatment, *$p<0.05$ and **$p<0.01$ by one way ANOVA and Tukey's *post hoc* tests.

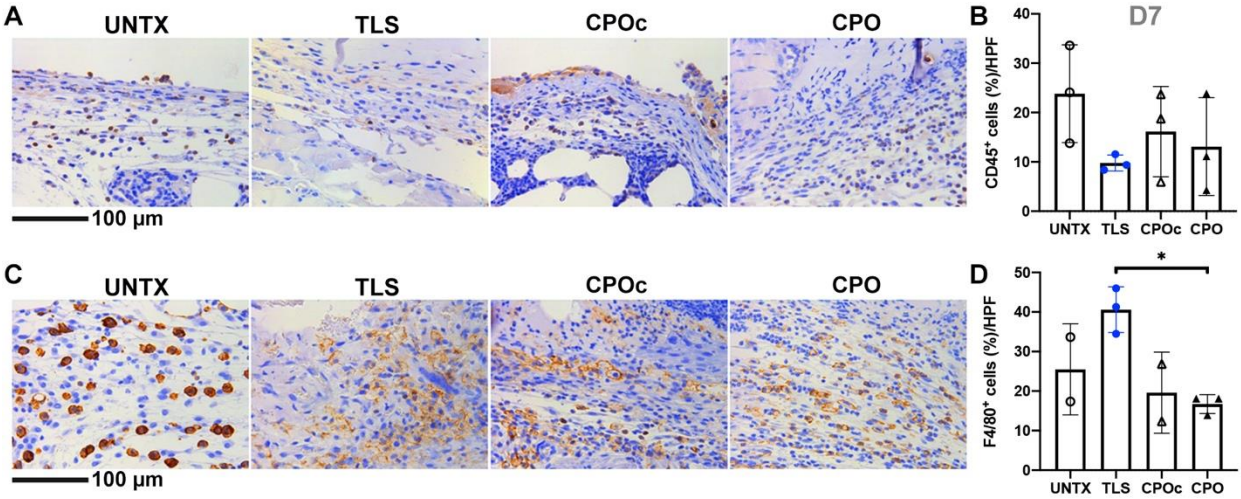

Figure 6. Inflammatory panel in db/db mouse wounds treated with lignin composite TLS, CPOc or CPO immediately post-wounding. Representative images of stained day 7 wound sections with antibodies against CD45 (A) and F4/80 (C). Scale bar = 250 µm. Quantification of % of $CD45^+$ (B) and $F4/80^+$ (D) cells in HPF in the wound sections showed no significant increase in inflammatory markers in CPOc or CPO wounds at day 7. Mean±SD, n=3 wounds per treatment, *$p<0.05$ by one way ANOVA and Tukey's *post hoc* tests.

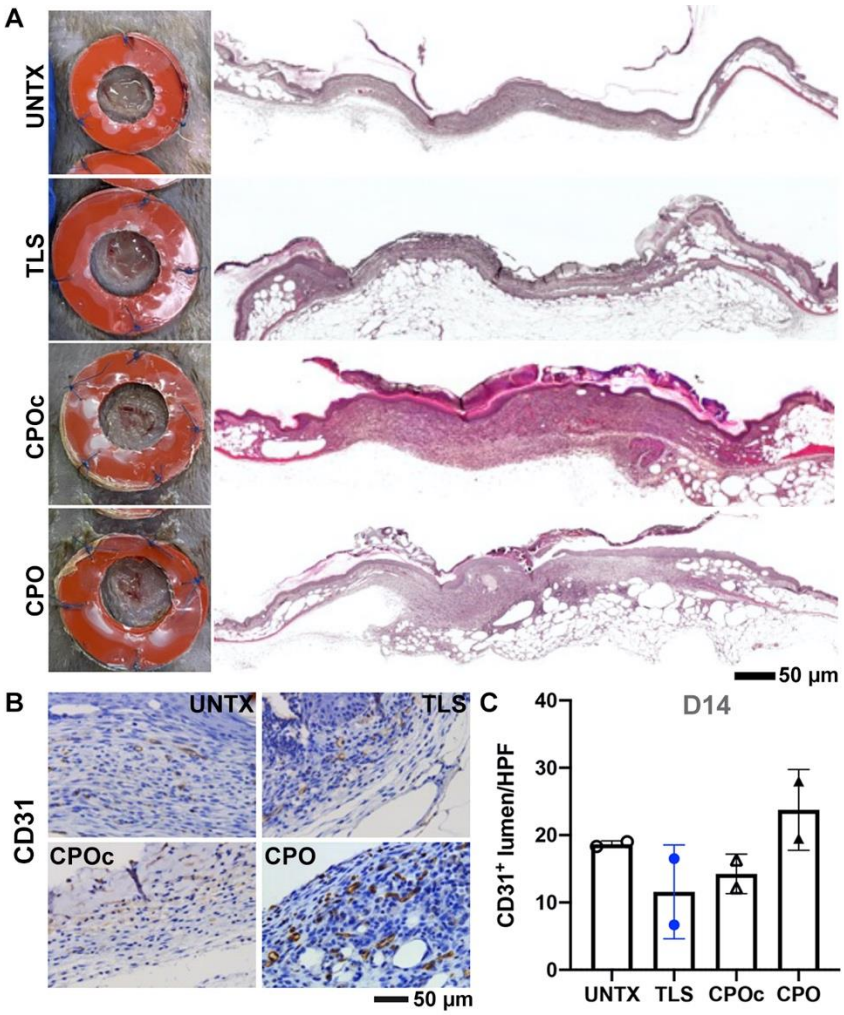

Figure 7. Healing progression of db/db mouse wounds treated with lignin composite TLS, CPOc or CPO immediately post-wounding. At 14 days post-wounding as compared to UNTX wounds. (A) Representative gross images taken at time of tissue collection at day 14 post-wounding shows improved healing in CPOc and CPO wounds, with representative H&E staining of the wound sections. Scale bar = 50 µm. (B) Staining of day 14 wound sections with antibodies against CD31. Scale bar = 50 µm. (C) Quantification of CD31+ lumens showed an increase in lumens in the CPO lignin composite treated group at day 14. Mean±SD, n=2 wounds per treatment.

REFERENCES

1. Sen, C.K., *Human Wounds and Its Burden: An Updated Compendium of Estimates.* Adv Wound Care (New Rochelle), 2019. **8**(2): p. 39-48.
2. Nussbaum, S.R., et al., *An Economic Evaluation of the Impact, Cost, and Medicare Policy Implications of Chronic Nonhealing Wounds.* Value Health, 2018. **21**(1): p. 27-32.
3. Glovaci, D., W. Fan, and N.D. Wong, *Epidemiology of Diabetes Mellitus and Cardiovascular Disease.* Curr Cardiol Rep, 2019. **21**(4): p. 21.
4. *New CDC report: More than 100 million Americans have diabetes or prediabetes*, in *Diabetes growth rate steady, adding to health care burden*. 2017, Centers for Disease Control and Prevention.
5. Falanga, V., *Wound healing and its impairment in the diabetic foot.* Lancet, 2005. **366**(9498): p. 1736-43.
6. Delamaire, M., et al., *Impaired leucocyte functions in diabetic patients.* Diabet Med, 1997. **14**(1): p. 29-34.
7. Wysocki, J., et al., *The influence of thymus extracts on the chemotaxis of polymorphonuclear neutrophils (PMN) from patients with insulin-dependent diabetes mellitus (IDD).* Thymus, 1992. **20**(1): p. 63-7.
8. Das, A., et al., *Engulfment of apoptotic cells by macrophages: a role of microRNA-21 in the resolution of wound inflammation.* J Immunol, 2014. **192**(3): p. 1120-9.
9. Trengove, N.J., et al., *Analysis of the acute and chronic wound environments: the role of proteases and their inhibitors.* Wound Repair Regen, 1999. **7**(6): p. 442-52.
10. Schafer, M. and S. Werner, *Oxidative stress in normal and impaired wound repair.* Pharmacol Res, 2008. **58**(2): p. 165-71.
11. Dunnill, C., et al., *Reactive oxygen species (ROS) and wound healing: the functional role of ROS and emerging ROS-modulating technologies for augmentation of the healing process.* Int Wound J, 2017. **14**(1): p. 89-96.
12. Nouvong, A., et al., *Reactive oxygen species and bacterial biofilms in diabetic wound healing.* Physiol Genomics, 2016. **48**(12): p. 889-896.
13. Sen, C.K. and S. Roy, *Redox signals in wound healing.* Biochim Biophys Acta, 2008. **1780**(11): p. 1348-61.
14. Hunt, T.K., et al., *Anaerobic metabolism and wound healing: an hypothesis for the initiation and cessation of collagen synthesis in wounds.* Am J Surg, 1978. **135**(3): p. 328-32.
15. Siwik, D.A., P.J. Pagano, and W.S. Colucci, *Oxidative stress regulates collagen synthesis and matrix metalloproteinase activity in cardiac fibroblasts.* Am J Physiol Cell Physiol, 2001. **280**(1): p. C53-60.
16. Sacks, D., et al., *Multisociety Consensus Quality Improvement Revised Consensus Statement for Endovascular Therapy of Acute Ischemic Stroke.* Int J Stroke, 2018. **13**(6): p. 612-632.
17. Kai, D., et al., *Sustainable and Antioxidant Lignin–Polyester Copolymers and Nanofibers for Potential Healthcare Applications.* ACS Sustainable Chemistry & Engineering, 2017. **5**(7): p. 6016-6025.
18. Hajihashemi, S., S. Rajabpoor, and I. Djalovic, *Antioxidant potential in Stevia rebaudiana callus in response to polyethylene glycol, paclobutrazol and gibberellin treatments.* Physiol Mol Biol Plants, 2018. **24**(2): p. 335-341.

19. Javed, R., et al., *PVP and PEG doped CuO nanoparticles are more biologically active: Antibacterial, antioxidant, antidiabetic and cytotoxic perspective.* Mater Sci Eng C Mater Biol Appl, 2017. **79**: p. 108-115.
20. Zeng, W., et al., *Antioxidant treatment enhances human mesenchymal stem cell anti-stress ability and therapeutic efficacy in an acute liver failure model.* Sci Rep, 2015. **5**: p. 11100.
21. Choe, G., et al., *Anti-oxidant activity reinforced reduced graphene oxide/alginate microgels: Mesenchymal stem cell encapsulation and regeneration of infarcted hearts.* Biomaterials, 2019. **225**: p. 119513.
22. Yang, W., et al., *Polyvinyl alcohol/chitosan hydrogels with enhanced antioxidant and antibacterial properties induced by lignin nanoparticles.* Carbohydrate Polymers, 2018. **181**: p. 275-284.
23. Sharma, S.K. and A.P. Singh, *In vitro antioxidant and free radical scavenging activity of Nardostachys jatamansi DC.* J Acupunct Meridian Stud, 2012. **5**(3): p. 112-8.
24. Thi, P.L., et al., *In situ forming and reactive oxygen species-scavenging gelatin hydrogels for enhancing wound healing efficacy.* Acta Biomater, 2020. **103**: p. 142-152.
25. Li, J., et al., *N-acetyl cysteine-loaded graphene oxide-collagen hybrid membrane for scarless wound healing.* Theranostics, 2019. **9**(20): p. 5839-5853.
26. Ninan, N., et al., *Antibacterial and Anti-Inflammatory pH-Responsive Tannic Acid-Carboxylated Agarose Composite Hydrogels for Wound Healing.* ACS Appl Mater Interfaces, 2016. **8**(42): p. 28511-28521.
27. Wu, H., et al., *Ceria nanocrystals decorated mesoporous silica nanoparticle based ROS-scavenging tissue adhesive for highly efficient regenerative wound healing.* Biomaterials, 2018. **151**: p. 66-77.
28. Hosgood, G., *Wound healing. The role of platelet-derived growth factor and transforming growth factor beta.* Vet Surg, 1993. **22**(6): p. 490-5.
29. Noack, R., *E. A. NEWSHOLME und C. START: REGULATION IN METABOLISM. 349 Seiten, 92 Abb., 57 Tab. John Wiley & Sons, London, New York, Sydney, Toronto 1973. Preis: 6.00 £.* Food / Nahrung, 1975. **19**(7): p. 616-617.
30. Li, Z., et al., *Injectable, highly flexible, and thermosensitive hydrogels capable of delivering superoxide dismutase.* Biomacromolecules, 2009. **10**(12): p. 3306-16.
31. Balaji, S., et al., *Tissue-engineered provisional matrix as a novel approach to enhance diabetic wound healing.* Wound Repair Regen, 2012. **20**(1): p. 15-27.
32. Cho, H., et al., *Diabetic wound healing in a MMP9-/- mouse model.* Wound Repair Regen, 2016. **24**(5): p. 829-840.
33. Cho, H., et al., *Regulation of endothelial cell activation and angiogenesis by injectable peptide nanofibers.* Acta Biomater, 2012. **8**(1): p. 154-64.
34. Hurley, J.R., et al., *Nanofiber Microenvironment Effectively Restores Angiogenic Potential of Diabetic Endothelial Cells.* Adv Wound Care (New Rochelle), 2014. **3**(11): p. 717-728.
35. Zhao, H., et al., *ROS-scavenging hydrogel to promote healing of bacteria infected diabetic wounds.* Biomaterials, 2020. **258**: p. 120286.
36. Harrison, B.S., et al., *Oxygen producing biomaterials for tissue regeneration.* Biomaterials, 2007. **28**(31): p. 4628-34.
37. Lee, M.H., et al., *Lignin-based barrier restricts pathogens to the infection site and confers resistance in plants.* Embo j, 2019. **38**(23): p. e101948.

38. Hasegawa, Y., et al., *Lignosulfonic acid promotes hypertrophy in 3T3-L1 cells without increasing lipid content and increases their 2-deoxyglucose uptake.* Asian-Australas J Anim Sci, 2017. **30**(1): p. 111-118.
39. Qiu, M., et al., *Lignosulfonic Acid Exhibits Broadly Anti-HIV-1 Activity – Potential as a Microbicide Candidate for the Prevention of HIV-1 Sexual Transmission.* PLOS ONE, 2012. **7**(4): p. e35906.
40. Gordts, S.C., et al., *The Low-Cost Compound Lignosulfonic Acid (LA) Exhibits Broad-Spectrum Anti-HIV and Anti-HSV Activity and Has Potential for Microbicidal Applications.* PLOS ONE, 2015. **10**(7): p. e0131219.
41. Huang, C., et al., *Unveiling the Structural Properties of Lignin–Carbohydrate Complexes in Bamboo Residues and Its Functionality as Antioxidants and Immunostimulants.* ACS Sustainable Chemistry & Engineering, 2018. **6**(9): p. 12522-12531.
42. Mehta, A.Y., et al., *Allosterism-based simultaneous, dual anticoagulant and antiplatelet action: allosteric inhibitor targeting the glycoprotein Ibα-binding and heparin-binding site of thrombin.* Journal of Thrombosis and Haemostasis, 2016. **14**(4): p. 828-838.
43. Oveissi, F., et al., *Tough and Processable Hydrogels Based on Lignin and Hydrophilic Polyurethane.* ACS Appl Bio Mater, 2018. **1**(6): p. 2073-2081.
44. Zhang, Y., et al., *Novel lignin-chitosan-PVA composite hydrogel for wound dressing.* Mater Sci Eng C Mater Biol Appl, 2019. **104**: p. 110002.
45. Mahata, D., et al., *Lignin-graft-Polyoxazoline Conjugated Triazole a Novel Anti-Infective Ointment to Control Persistent Inflammation.* Sci Rep, 2017. **7**: p. 46412.
46. Xu, J., et al., *Lignin-Incorporated Nanogel Serving As an Antioxidant Biomaterial for Wound Healing.* ACS Appl Bio Mater, 2021. **4**(1): p. 3-13.
47. Jaiswal, L., et al., *Lignin-mediated green synthesis of AgNPs in carrageenan matrix for wound dressing applications.* Int J Biol Macromol, 2020. **159**: p. 859-869.
48. Dizhbite, T., et al., *Characterization of the radical scavenging activity of lignins--natural antioxidants.* Bioresour Technol, 2004. **95**(3): p. 309-17.
49. Pan, X., et al., *Organosolv ethanol lignin from hybrid poplar as a radical scavenger: Relationship between lignin structure, extraction conditions, and antioxidant activity.* J. Agric. Food Chem., 2006. **54**: p. 5806−5813.
50. Kedare, S.B. and R.P. Singh, *Genesis and development of DPPH method of antioxidant assay.* J Food Sci Technol, 2011. **48**(4): p. 412-22.
51. Samuel, E.L.G., et al., *Hydrophilic carbon clusters as therapeutic, high-capacity antioxidants.* Trends in biotechnology, 2014. **32**(10): p. 501-505.
52. Baba, S.A. and S.A. Malik, *Determination of total phenolic and flavonoid content, antimicrobial and antioxidant activity of a root extract of Arisaema jacquemontii Blume.* Journal of Taibah University for Science, 2015. **9**(4): p. 449-454.
53. Kai, D., et al., *Engineering Poly(Lactide)–Lignin Nanofibers with Antioxidant Activity for Biomedical Application.* ACS Sustainable Chem. Eng., 2016. **4**(10): p. 5268.
54. Wang, J., et al., *Engineering PCL/lignin nanofibers as an antioxidant scaffold for the growth of neuron and Schwann cell.* Colloids Surf B Biointerfaces, 2018. **169**: p. 356-365.
55. Das, B., et al., *In Vivo Cell Tracking, Reactive Oxygen Species Scavenging, and Antioxidative Gene Down Regulation by Long-Term Exposure of Biomass-Derived Carbon Dots.* ACS Biomaterials Science & Engineering, 2019. **5**(1): p. 346-356.
56. Liu, R., et al., *Lignin-Based Micro- and Nanomaterials and their Composites in Biomedical Applications.* ChemSusChem, 2020. **13**(17): p. 4266-4283.

57. Belgodere, J.A., et al., *Attenuating Fibrotic Markers of Patient-Derived Dermal Fibroblasts by Thiolated Lignin Composites.* ACS Biomater Sci Eng, 2021. **7**(6): p. 2212-2218.
58. Belgodere, J.A., et al., *Modulating Mechanical Properties of Collagen-Lignin Composites.* ACS Appl Bio Mater, 2019. **2**(8): p. 3562-3572.
59. Balaji, S., et al., *Engineering Antioxidant and Oxygen-Releasing Lignin Composites to Accelerate Wound Healing.* bioRxiv, 2022: p. 2022.03.18.484913.
60. Carpentier, G., et al., *Angiogenesis Analyzer for ImageJ - A comparative morphometric analysis of "Endothelial Tube Formation Assay" and "Fibrin Bead Assay".* Sci Rep, 2020. **10**(1): p. 11568.
61. Keswani, S.G., et al., *Adenoviral mediated gene transfer of PDGF-B enhances wound healing in type I and type II diabetic wounds.* Wound Repair Regen, 2004. **12**(5): p. 497-504.
62. Cano Sanchez, M., et al., *Targeting Oxidative Stress and Mitochondrial Dysfunction in the Treatment of Impaired Wound Healing: A Systematic Review.* Antioxidants (Basel), 2018. **7**(8).
63. Dworzański, J., et al., *Glutathione peroxidase (GPx) and superoxide dismutase (SOD) activity in patients with diabetes mellitus type 2 infected with Epstein-Barr virus.* PLoS One, 2020. **15**(3): p. e0230374.
64. Lan, C.C., et al., *High-glucose environment enhanced oxidative stress and increased interleukin-8 secretion from keratinocytes: new insights into impaired diabetic wound healing.* Diabetes, 2013. **62**(7): p. 2530-8.
65. Waldron, A.L., et al., *Oxidative stress-dependent MMP-13 activity underlies glucose neurotoxicity.* J Diabetes Complications, 2018. **32**(3): p. 249-257.
66. Kim, J.H., et al., *High Levels of Oxidative Stress and Skin Microbiome are Critical for Initiation and Development of Chronic Wounds in Diabetic Mice.* Sci Rep, 2019. **9**(1): p. 19318.
67. Goldin, A., et al., *Advanced glycation end products: sparking the development of diabetic vascular injury.* Circulation, 2006. **114**(6): p. 597-605.
68. Boulton, A.J.M., et al., in *Diagnosis and Management of Diabetic Foot Infections*. 2020, American Diabetes Association: Arlington (VA).
69. Targosz-Korecka, M., et al., *Stiffness memory of EA.hy926 endothelial cells in response to chronic hyperglycemia.* Cardiovasc Diabetol, 2013. **12**: p. 96.
70. Costantino, S., F. Paneni, and F. Cosentino, *Hyperglycemia: a bad signature on the vascular system.* Cardiovasc Diagn Ther, 2015. **5**(5): p. 403-6.
71. Jin, G., et al., *mRNAs expression profiles of high glucose-induced memory in human umbilical vein endothelial cells.* Diabetes Metab Syndr Obes, 2019. **12**: p. 1249-1261.
72. Nathan, D.M., et al., *Intensive diabetes treatment and cardiovascular disease in patients with type 1 diabetes.* N Engl J Med, 2005. **353**(25): p. 2643-53.
73. Thiem, K., et al., *Hyperglycemic Memory of Innate Immune Cells Promotes In Vitro Proinflammatory Responses of Human Monocytes and Murine Macrophages.* J Immunol, 2021. **206**(4): p. 807-813.
74. Li, J., et al., *Inhibition of reactive oxygen species by Lovastatin downregulates vascular endothelial growth factor expression and ameliorates blood-retinal barrier breakdown in db/db mice: role of NADPH oxidase 4.* Diabetes, 2010. **59**(6): p. 1528-38.

75. Gonzalez-Pacheco, F.R., et al., *Mechanisms of endothelial response to oxidative aggression: protective role of autologous VEGF and induction of VEGFR2 by H2O2.* Am J Physiol Heart Circ Physiol, 2006. **291**(3): p. H1395-401.
76. Folkman, J., et al., *Isolation of a tumor factor responsible for angiogenesis.* J Exp Med, 1971. **133**(2): p. 275-88.
77. Leung, D.W., et al., *Vascular endothelial growth factor is a secreted angiogenic mitogen.* Science, 1989. **246**(4935): p. 1306-9.
78. Yano, K., L.F. Brown, and M. Detmar, *Control of hair growth and follicle size by VEGF-mediated angiogenesis.* J Clin Invest, 2001. **107**(4): p. 409-17.
79. Zhang, Y., H. Matsuo, and E. Morita, *Increased production of vascular endothelial growth factor in the lesions of atopic dermatitis.* Arch Dermatol Res, 2006. **297**(9): p. 425-9.
80. Genovese, A., et al., *Angiogenesis, lymphangiogenesis and atopic dermatitis.* Chem Immunol Allergy, 2012. **96**: p. 50-60.
81. Detoraki, A., et al., *Vascular endothelial growth factors synthesized by human lung mast cells exert angiogenic effects.* J Allergy Clin Immunol, 2009. **123**(5): p. 1142-9, 1149.e1-5.
82. Lee, J., et al., *Inhibition of Hippo Signaling Improves Skin Lesions in a Rosacea-Like Mouse Model.* Int J Mol Sci, 2021. **22**(2).
83. Rossiter, H., et al., *Loss of vascular endothelial growth factor a activity in murine epidermal keratinocytes delays wound healing and inhibits tumor formation.* Cancer Res, 2004. **64**(10): p. 3508-16.
84. Larcher, F., et al., *VEGF/VPF overexpression in skin of transgenic mice induces angiogenesis, vascular hyperpermeability and accelerated tumor development.* Oncogene, 1998. **17**(3): p. 303-11.
85. Levy, A.P., et al., *Transcriptional regulation of the rat vascular endothelial growth factor gene by hypoxia.* J Biol Chem, 1995. **270**(22): p. 13333-40.
86. Forsythe, J.A., et al., *Activation of vascular endothelial growth factor gene transcription by hypoxia-inducible factor 1.* Mol Cell Biol, 1996. **16**(9): p. 4604-13.
87. Mazure, N.M., et al., *Induction of vascular endothelial growth factor by hypoxia is modulated by a phosphatidylinositol 3-kinase/Akt signaling pathway in Ha-ras-transformed cells through a hypoxia inducible factor-1 transcriptional element.* Blood, 1997. **90**(9): p. 3322-31.
88. Sheikh, A.Y., et al., *Effect of hyperoxia on vascular endothelial growth factor levels in a wound model.* Arch Surg, 2000. **135**(11): p. 1293-7.
89. Martinez-Ferrer, M., et al., *Dermal transforming growth factor-beta responsiveness mediates wound contraction and epithelial closure.* Am J Pathol, 2010. **176**(1): p. 98-107.
90. Nguyen, P.D., et al., *Improved diabetic wound healing through topical silencing of p53 is associated with augmented vasculogenic mediators.* Wound Repair Regen, 2010. **18**(6): p. 553-9.